

Figure 3. Variation of scaled expansion factor $\alpha_s^3 |\tau| M_w^{1/2}$ of hydrodynamic size as a function of scaled reduced temperature $|\tau| M_w^{1/2}$. Data points (\diamond and \star) of the high molecular weight PS sample, as listed in Table III, are plotted in Figure 17 of ref 8 for comparison. Filled symbols denote "metastable" collapsed regime.

reached the asymptotic height and belonged to the metastable collapsed regime (emphasized by the filled symbols).

In summary, (1) degradation of very long polymer chains occurs readily at very dilute polymer concentrations ($C \leq 10^{-6}$ g/g) for our high molecular weight PS sample. (2) In coil-to-globule transition studies, the polydispersity effect becomes a critical issue. As it is difficult to prepare ultrahigh molecular weight PS samples with a very narrow molecular weight distribution, the advantage of this ultrahigh molecular weight PS sample was overshadowed by its unexpectedly broad polydispersity. (3) Most of the experiments suggested measurements in the metastable collapsed regime at finite concentrations.

The present experiment simply demonstrates polymer solution behavior in the metastable region and conforms to problems associated with earlier results in the literature. As the low polymer concentration (left) side of the cloud-point curve is not only very steep but also occurs at very low polymer concentrations, it becomes essential that the only accessible path to reach the globule state is to use a ultrahigh molecular weight polymer with a very narrow molecular weight distribution.

Acknowledgment. B.C. gratefully acknowledges support of this work by the National Science Foundation (Polymers Program, DMR 8617820).

Registry No. PS, 9003-53-6.

References and Notes

- (1) Williams, C.; Brochard, F.; Frisch, H. L. *Annu. Rev. Phys. Chem.* **1981**, *32*, 433 and references cited therein.
- (2) DiMarzio, E. A. *Macromolecules* **1984**, *17*, 969.
- (3) Kholodenko, A. L.; Freed, K. F. *J. Chem. Phys.* **1985**, *80*, 900.
- (4) Allegra, G.; Ganazzoli, F. *J. Chem. Phys.* **1985**, *83*, 397.
- (5) Vidakovic, P.; Rondelez, F. *Macromolecules* **1984**, *17*, 418 and references cited therein.
- (6) de Gennes, P.-G. *J. Phys. Lett.* **1978**, *39*, 299.
- (7) Akcasu, A. Z.; Han, C. C. *Macromolecules* **1979**, *12*, 276.
- (8) Park, I. H.; Wang, Q.-W.; Chu, B. *Macromolecules* **1987**, *20*, 1965.
- (9) Chu, B.; Park, I. H.; Wang, Q.-W.; Wu, C. *Macromolecules* **1987**, *20*, 2833.
- (10) Chu, B. *J. Polym. Sci., Polym. Symp.* **1985**, *73*, 137.
- (11) *Light Scattering from Polymer Solutions*; Huglin, M. B., Ed.; Academic: New York, 1972.
- (12) Miyaki, Y.; Einaga, Y.; Fujita, H. *Macromolecules* **1978**, *11*, 1180.
- (13) Koppel, D. E. *J. Chem. Phys.* **1972**, *57*, 4814.
- (14) Brown, J. C.; Pusey, P. N. *J. Phys. D.* **1974**, *7*, 31.
- (15) Chu, B.; Onclin, M.; Ford, J. R. *J. Phys. Chem.* **1984**, *88*, 6566.
- (16) Slagowski, E.; Tsai, B.; McIntyre, D. *Macromolecules* **1976**, *9*, 687.

Communications to the Editor

Time-Resolved SAXS on Crystallization of a Low-Density Polyethylene/High-Density Polyethylene Polymer Blend

Small-angle X-ray scattering (SAXS) has been used successfully to study the structure of polymer blends.¹⁻⁵ A natural extension is to use synchrotron radiation for measurements of time-resolved structural changes during early stages of crystallization.⁶⁻⁸ In this paper, we report our time-resolved SAXS patterns of a blend of low-density polyethylene (LDPE) and high-density polyethylene (HDPE) and of the respective homopolymers.

HDPE has $M_w = 1.60 \times 10^5$ g/mol, $M_w/M_n = 7.1$, ca. one short chain branching per 1000 carbon atoms, and a density of 0.957 g/mL. The LDPE has $M_w = 2.86 \times 10^5$ g/mol, $M_w/M_n = 16$, ~ 26 short chains branching per 1000 carbon atoms, and a density of 0.920 g/mL. The blend is 50/50 of HDPE and LDPE by weight percentage. These are the same materials as used in a previous study.⁵

SAXS measurements were carried out by using a modified Kratky collimator⁹ adapted for synchrotron radiation at the SUNY beamline, NSLS, Brookhaven National Laboratory (BNL). The wavelength of X-ray used was 0.154 nm. We used a photodiode array of ~ 2.5 -cm window length as the linear position sensitive detector, which was mounted at a distance of 548 mm from the sample.

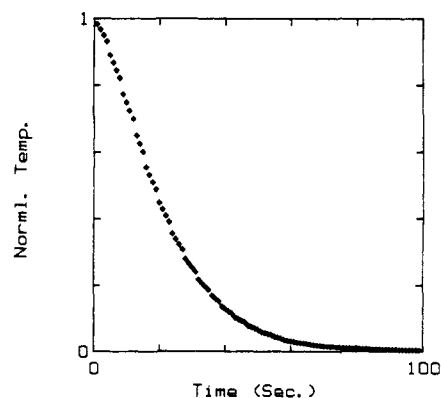


Figure 1. Cooling curve during a temperature jump ΔT of 70 °C. The temperature was normalized by $(T - T_2)/(T_1 - T_2)$. T_1 and T_2 denote the temperatures of the thermal blocks.

In order to achieve rapid cooling during the SAXS measurements, the copper cell containing the polymer sample was quickly moved from one thermal block ($T = T_1$) to the other block ($T = T_2$) by use of a pneumatic piston. The cooling rate depends on the temperature difference between the two thermal blocks ($\Delta T = T_1 - T_2$). For example, as shown in Figure 1, the cooling rate achieved during the first 30 s, after a temperature jump

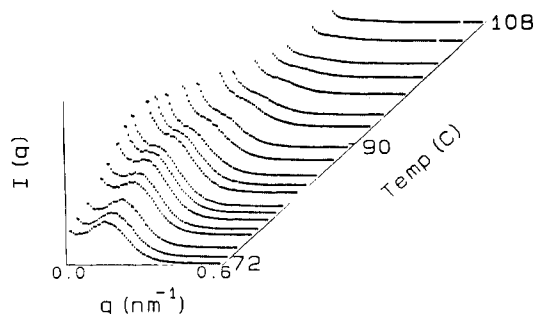


Figure 2. Typical time-resolved SAXS intensity profiles of HDPE during a temperature jump from 135 to 65 °C ($\Delta T = 70$ °C). Each curve has been collected for 0.5 s and corrected for detector nonuniformity, background, and absorption.

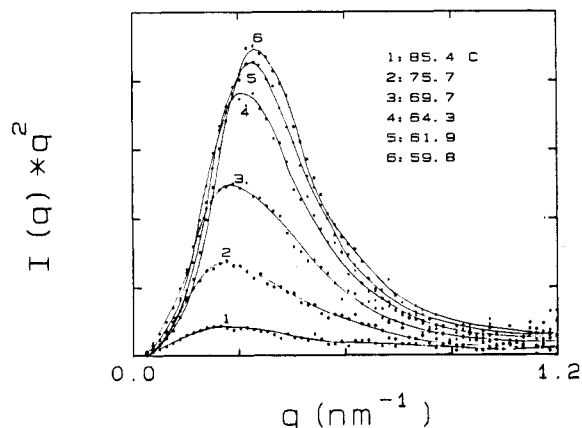


Figure 3. Lorentz-corrected SAXS intensities of LDPE measured during a temperature jump from 120 to 50 °C. Each curve has been collected for 0.5 s and corrected for detector nonuniformity, background, and absorption.

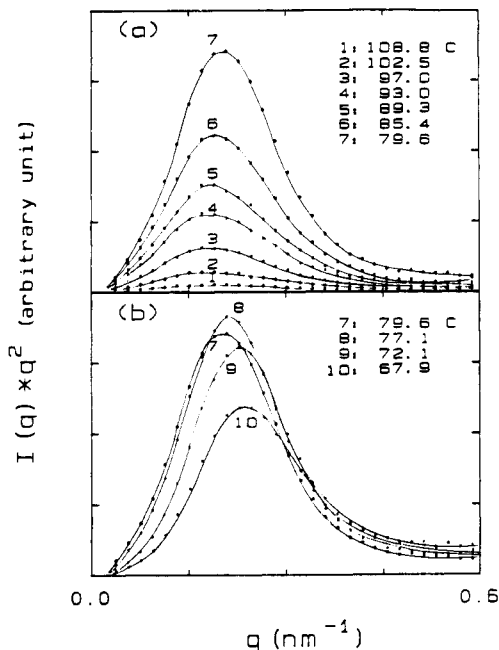


Figure 4. Lorentz-corrected SAXS intensities of HDPE measured during a temperature jump from 135 to 65 °C. The curves are partitioned into two stages, (a) and (b), for the sake of clarity. Note the peak shift at the later stage, (b), of crystallization.

(ΔT) of 70 °C, was ~ 110 °C/min.

Figure 2 shows typical time-resolved SAXS intensity profiles of HDPE during rapid cooling from 135 to 65 °C. Each curve was measured for a 0.5-s period and the total time span of the experiment (from 108 to 72 °C) was 20 s.

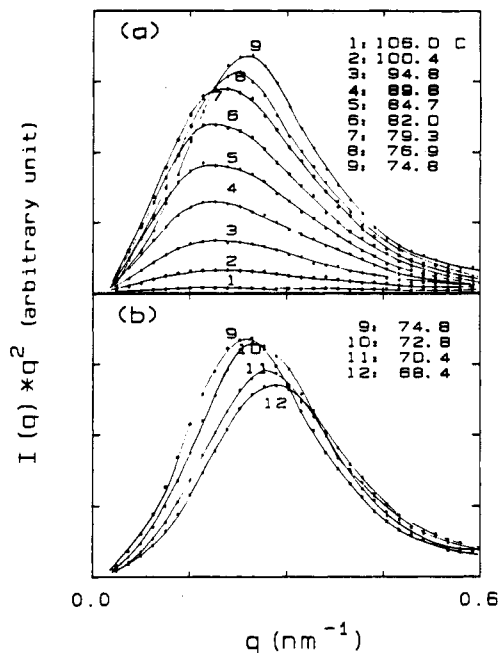


Figure 5. Lorentz-corrected SAXS intensities of 50/50 blend measured during a temperature jump from 135 to 65 °C. The curves are partitioned into two stages, (a) and (b), for the sake of clarity.

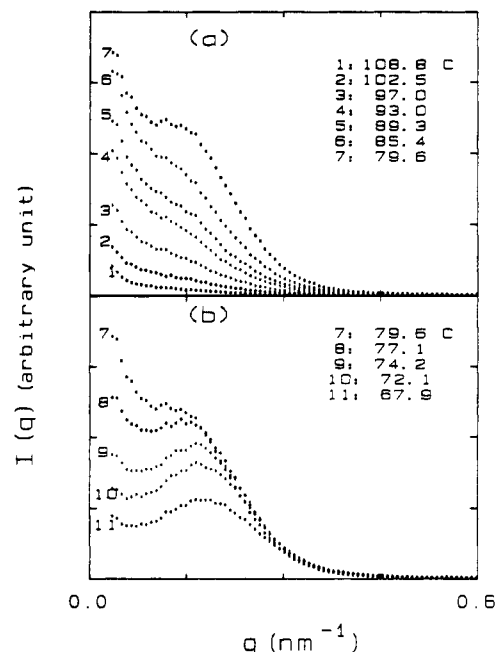


Figure 6. Same intensities of HDPE as plotted in Figure 4 but without Lorentz correction.

A Lorentz factor correction was made to each scattering curve. The corrected intensities ($I(q) \cdot q^2$) are shown in Figure 3 (LDPE), Figure 4 (HDPE), and Figure 5 (50/50 blend of LDPE and HDPE). All three samples were crystallized under the same cooling rate with $\Delta T = 70$ °C. The LDPE sample was cooled from 120 to 50 °C while the blend was from 135 to 65 °C. SAXS curves from HDPE, LDPE, and the 50/50 blend show a single reflection and share similar features. As shown in Figures 3–5, the maximum, whose position and width are determined by characteristics of the lamella structure, increases in height upon cooling and then subsequently changes its position to a lower spacing. In fact, such a peak shift occurs when the marked hump starts to appear in the original scattering pattern as shown in Figure 6. Such changes in the scat-

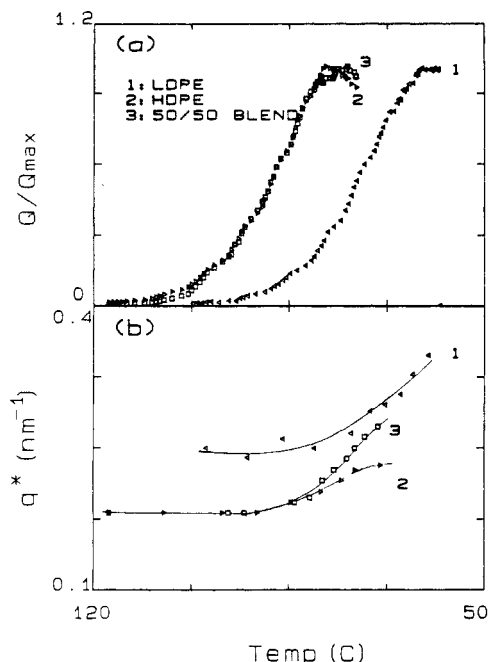


Figure 7. (a) Plot of integrated intensities, Q , normalized by the maximum, Q_{\max} , versus temperature; (b) peak position change in the scattering pattern due to crystallization upon cooling.

tering pattern during crystallization have been noted by Schultz et al.^{10,11} They viewed the changes as a transition from single particle scattering to an interference pattern. However, as is apparent in the scattering curves in Figure 3-5, the intensities, $I(q) \cdot q^2$, shall not yield a straight line using the Guinier plot. We suggest that the scattering pattern change could be the reflection of structural changes from a disordered lamella structure with a very broad distribution of lamella spacing and large amounts of amorphous gap to well-defined lamella stacks. The crystallization of polyethylene from a melt state can be described by two stages: (1) growing of spherulites to fill the entire volume and (2) creation of new crystallites or thickening of existing crystallites within the spherulites. The early period of crystallization would be dominated by the first stage and later period by the second stage. In a rapid crystallization process, the lamella structure created during the first stage would probably be disordered and contain a large amount of amorphous gaps between the lamella stacking. Such disordered lamella stacks may not be regular enough to produce a hump in the scattering profile.¹² However, the structure transforms into a regularly stacked lamella as new crystallites fill in the amorphous gaps during the second stage of crystallization, thus producing a marked Bragg reflection peak.

The integrated intensities normalized by a maximum, Q/Q_{\max} , and the peak positions in q , q^* , as shown in Figures 3-5 for LDPE, HDPE, and 50/50 blend are plotted against the temperature in parts a and b of Figure 7, respectively. The integrated intensity, Q , for a two-phase system (crystal and amorphous) is given¹³ by

$$Q = 4\pi \int q^2 I(q) dq = 8\pi^3 (\rho_c - \rho_a)^2 \alpha (1 - \alpha) \quad (1)$$

where ρ_c and ρ_a are the densities of crystalline and amorphous region and α denotes the degree of crystallinity. As shown in Figure 7, HDPE and LDPE seem to share a similar kinetic behavior except for the difference in crystallization temperature. It is interesting to note that the two curves for HDPE and 50/50 blend overlap each other until they reach the maximum. This result suggests that the HDPE component in the blend dominates the crys-

tallization process during the early stage and the kinetic process is hardly affected by the LDPE component. The LDPE would separate out to form amorphous gaps between the lamella stacking formed mainly by the HDPE component. The curves in Figure 6b suggest such a supposition. HDPE and the 50/50 blend show an equivalent lamella spacing down to $\sim 85^\circ\text{C}$ and then begin to diverge to have different peak positions reflecting different lamella spacings. HDPE and the 50/50 blend show an equivalent lamella spacing down to $\sim 85^\circ\text{C}$ and then begin to diverge to have different peak positions reflecting different lamella spacings. HDPE and the 50/50 blend show an equivalent lamella spacing down to $\sim 85^\circ\text{C}$ and then begin to diverge to have different peak positions reflecting different lamella spacings. HDPE and the 50/50 blend show an equivalent lamella spacing down to $\sim 85^\circ\text{C}$ and then begin to diverge to have different peak positions reflecting different lamella spacings. HDPE and the 50/50 blend show an equivalent lamella spacing down to $\sim 85^\circ\text{C}$ and then begin to diverge to have different peak positions reflecting different lamella spacings.

In conclusion, the fine structural changes during the early stage of crystallization, observed through SAXS with synchrotron radiation, have suggested the following clues. The single Bragg reflection does not necessarily mean that the two components have cocrystallized to form a single lamella structure, as has been interpreted previously. The observation could be interpreted as a separation between the two (LDPE/HDPE) components on an interlamella scale. A more detailed study is under way.

Acknowledgment. B.C. gratefully acknowledges support of this research by the U.S. Department of Energy (DEFG0286-ER45237A001). The work was carried out at the SUNY beamline supported by the U.S. Department of Energy (DEFG0286-ER45231A001) at the National Synchrotron Light Source, Brookhaven National Laboratory, which is sponsored by the U.S. Department of Energy under contract (DE-AC02-76CH00016).

Registry No. HDPE, 9002-88-4.

References and Notes

- (1) Smith, P.; Manley, R. *Macromolecules* **1979**, *12*, 483.
- (2) Hu, S. R.; Kyu, T.; Stein, R. S. *J. Polym. Sci., Polym. Phys. Ed.* **1987**, *25*, 71.
- (3) Kyu, T.; Hu, S. R.; Stein, R. S. *J. Polym. Sci., Polym. Phys. Ed.* **1987**, *25*, 89.
- (4) Ree, M.; Kyu, T.; Stein, R. S. *J. Polym. Sci., Polym. Phys. Ed.* **1987**, *25*, 105.
- (5) Ree, M. Ph.D. Thesis, University of Massachusetts, 1987.
- (6) Russell, T. P.; Koberstein, J. T. *J. Polym. Sci., Polym. Phys. Ed.* **1985**, *23*, 1109.
- (7) Elsnor, G.; Riekel, C.; Zachmann, H. G. *Adv. Polym. Sci.* **1985**, *67*, 1.
- (8) Ungar, G.; Keller, A.; *Polymer* **1986**, *27*, 1835.
- (9) Chu, B.; Wu, D.-Q.; Wu, C. *Rev. Sci. Instrum.* **1987**, *58*, 1158.
- (10) Schultz, J. M. *J. Polym. Sci., Polym. Phys. Ed.* **1976**, *14*, 2291.
- (11) Schultz, J. M.; Hendricks, R. W. *J. Appl. Crystallogr.* **1978**, *11*, 551.
- (12) Vonk, C. G. *J. Appl. Crystallogr.* **1978**, *11*, 541.
- (13) Guinier, A.; Fournier, G. *Small Angle Scattering of X-Rays*; Wiley: New York, 1955.

* Author to whom correspondence should be addressed.

[†] State University of New York at Stony Brook.

[‡] University of Massachusetts.

[§] State University of New York at Buffalo.

[‡] SUNY X3 Beamline.

H. H. Song,[†] R. S. Stein,[‡] D.-Q. Wu,[†] M. Ree,[‡]
J. C. Phillips,^{§,‡} A. LeGrand,[‡] and B. Chu^{*,†}

Chemistry Department
State University of New York at Stony Brook
Stony Brook, New York 11794-3400

Department of Polymer Science and Engineering
University of Massachusetts
Amherst, Massachusetts 01003

Chemistry Department
State University of New York at Buffalo
Buffalo, New York 14214

SUNY X3 Beamline, NSLS
Brookhaven National Laboratory, Upton, New York 11973

Received January 14, 1988